Ultra-Small Imaging and Spectroscopic Elements with Subwavelength Performance

Kevin J. Webb and Shivanand
School of Electrical and Computer Engineering, Purdue University
465 Northwestern Ave, West Lafayette, IN 47907-2314
webb@purdue.edu

July 26, 2007

Abstract

Ag/SiO_2 and Au/Si multilayer imaging structures are shown to have subwavelength imaging performance. The influence of the duty cycle is presented. Imaging possibilities with a slab having isotropic negative effective dielectric constant is also explored. This system may be worthy of an experimental program to establish that subwavelength resolution is practical. Success will lead to a new class of imaging, memory, and interconnection structures.

1 Introduction

Conventional optics suffers from the diffraction limit because only the propagating components of the plane wave spectrum are available. As a consequence, the spot size is limited to about one wavelength. There is therefore a link between memory density and wavelength, for example. Information about the subwavelength features of the object are carried by the evanescent waves, which decay exponentially. A negative refractive index slab can act as a lens because of negative refraction, and of particular interest, can amplify the evanescent fields and produce images with subwavelength features [1, 2, 3, 4]. The primary features which negative index materials (NIMs) offer are: negative refraction, evanescent field growth, leading to the prospect of subwavelength imaging, and dispersion. These characteristics, individually and collectively, are important for imaging and a variety of other optical signal processing applications, in which an incident field (or set of fields) is transformed in some manner at the output (such as to a subwavelength spot). While building negative index materials at optical wavelengths will be very challenging, achieving low-loss structures which perform the aforementioned operations is possible now.

We have shown that a layered metal-insulator stack has the capability of subwavelength imaging [5]. It works because the effective dielectric constant is anisotropic and hence the structure converts evanescent fields from the source (the object) to propagating wave the multi-layer stack. In this way, information about the evanescent fields from the source can be conveyed to the image plane. Here we present an investigation of the multilayer Ag-SiO_2 film system that provides subwavelength spot resolution.

Photonic crystals have been shown to exhibit negative refraction [6, 7]. However, why constrain the problem to be regular (periodic)? In doing so, there are few variables (e.g., material, period, and duty cycle, as in a photonic crystal) to achieve particular field transformations. We have shown that irregular structures having many degrees of freedom allow both high performance field transformations and new functions [8, 4, 9, 10]. Control over the evanescent fields is essential in achieving such small focus regions. While the designs require nonlinear optimization, structures can be achieved which provide NIM features. Another important aspect of the planned

work is to design and build very small elements that function as spectrometers, an extension of some preliminary work we have done [10].

2 Results

2.1 Metal/Dielectric system (Anisotropic effective dielectric constant)

We explore the near-field imaging properties of a multilayered metal and dielectric system with an emphasis on the role of the available variables, namely, the duty cycle (D) and the number of layers. The slab structure we consider is composed of alternating layers of metal and dielectric and is surrounded by free space, as shown in Figure 1(a). The incident plane is defined as being at the left side of the slab, with the other side being the transmission plane, which is also the imaging plane. The total metal thickness divided by the slab thickness gives D. The metal (relative) dielectric constant is $\epsilon_- = \epsilon'_- + i\epsilon''_-$, with $\epsilon'_- < 0$, and that for the dielectric $\epsilon_+ = \epsilon'_+ + i\epsilon''_+$.

An effective medium dielectric constant can be defined under the quasi-static approximation, provided that the wavelength is large relative to the period and that there are a sufficient number of periods. From the spatial average, referring to Figure 1(a), and assuming continuity of the tangential electric field, $\epsilon_x = (\epsilon_- D + \epsilon_+(1-D))$, and from the continuity of the electric flux density normal to the layers, $\epsilon_z^{-1} = \left(\epsilon_-^{-1} D + \epsilon_+^{-1}(1-D)\right)$. For the TM field ($H_y$, E_x, E_z), the dispersion relation for the anisotropic slab defined by ϵ_x and ϵ_z is $k_x^2\epsilon_z^{-1} + k_z^2\epsilon_x^{-1} = k_0^2$, where in free space $k_0^2 = \omega^2 c^2 = k_x^2 + k_{z0}^2$ and c is the light speed. For a multi-layer slab of total thickness d, operating in the effective medium regime, the plane wave transmission coefficient (with $\exp(i\omega t)$) is

$$T(k_x) \;=\; \frac{(1-r^2)\exp(-ik_z d)}{1 - r^2\exp(-i2k_z d)}, \tag{1}$$

where r is the reflection coefficient for the TM mode. A perfect lens has $T(k_x) = 1$.

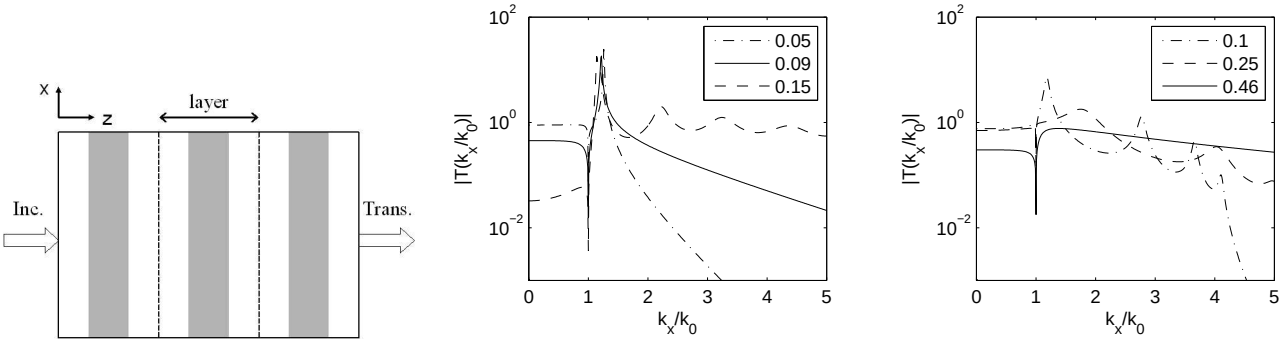

(a) (b) (c)

Figure 1: (a) Schematic of a 3-layer metal (gray) / dielectric (white) structure. Metal is placed at the center of each layer. The transmission spectrum with varying duty cycle for (b) Ag/SiO_2 and (c) Au/Si multilayered slab, in the effective medium regime. The slab is 400 nm thick, and the free space wavelength is λ_0=700 nm. k_0 is the free space wave number, and $|T|$ is the magnitude of the transmission coefficient across the slab.

Figure 1(b) and Fig. 1(c) show the variation of the magnitude of the transmission coefficient with the duty cycle in the effective medium regime at λ_0=700 nm for a 400 nm thick slab of Ag/SiO_2 and Au/Si, respectively. With increasing D, the amplitude of $|T|$ decreases for propagating fields ($k_x/k_0 < 1$) but increases for evanescent fields ($k_x/k_0 > 1$). It is clearly possible to adjust the parameters of the stack to achieve good magnitude and phase transfer

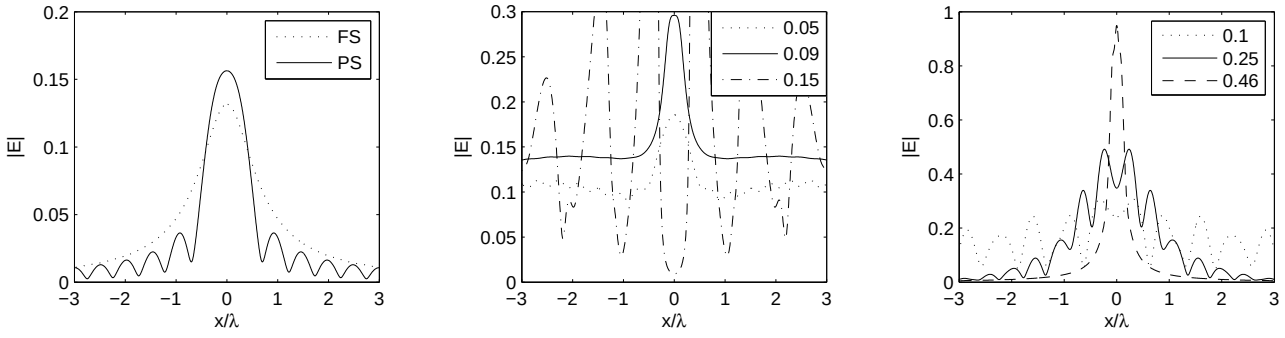

(a) (b) (c)

Figure 2: The magnitude of total electric field $|E|$ for a wavelength of $\lambda_0 = 700$ nm for a single object of width $0.1\lambda_0$. (a) FS is the image obtained after free space propagation over a distance of 400 nm. PS is the propagation spectrum determined from the object plane-wave expansion with the evanescent field removed, which is the perfect far-field imaging result with a positive index lens. Variation of the magnitude of total electric field $|E|$ at the image plane with the duty cycle for a 400 nm thick: (b)Ag/SiO_2 slab and (c)Au/Si slab, in the effective medium regime.

function characteristics. However, one could expect that the optimal design will depend on the particular object to be imaged.

We consider the example of a TM incident field having $H_y = 1$ within a strip of width 0.1 λ_0, being representative of a small aperture that may be a transmitting source or a feature on a lithographic mask. This object field is then imaged by means of a multilayer slab structure of total thickness 400 nm, so the image plane is removed from the object plane by this distance. An exact analytical solution is possible for this slab geometry. A plane wave expansion was used to solve for H_y in each region, and the electric field $\mathbf{E}$ was determined from an inverse Fourier transform of the plane-wave spectrum for H_y (each plane wave component is multiplied by its respective impedance).

Figure 2 shows the magnitude of the total electric field $|E|$ as a function of position at the image plane for a wavelength of λ_0=700 nm. Figure 2(a) gives the result for the propagating spectrum (PS), which was determined from the object-plane-wave expansion with the evanescent fields removed, as well as the free space (FS) result for propagation over 400 nm. We consider these as important reference results. We studied two different metal/dielectric slabs in the effective medium regime. The result for a Ag/SiO_2 slab in shown in Fig. 2(b) and that for a Au/Si slab in Fig. 2(c). As compared to both free space propagation and the propagating spectrum results, the layered structure can provide an improved image with parameter tuning. The best full width half maximum (FWHM) images are approximately $0.3\lambda_0$ for Au/Si and $0.9\lambda_0$ for Ag/SiO_2.

2.2 Negative Isotropic Dielectric Constant

We consider a single slab of material with isotropic $\epsilon = \epsilon' + i\epsilon''$, and with $\epsilon' < 0$. This condition is satisfied, for example, by metals at optical frequencies. It is possible to synthesize materials that have these properties, such as mixtures of metals and dielectrics, and fabrication can be relatively straight forward. This motivates us to evaluate the imaging prospects of a negative dielectric constant slab.

Figure 3(a) shows the transmission spectrum obtained for three different negative dielectric constants for $\lambda_0 = 700$ nm and a 400 nm thick slab. For propagating waves ($k_x/k_0 < 1$), the amplitude of transmission coefficient decreases with more negative ϵ'. The resonant peak in the evanescent field transfer function can be very prominent and approaches $k_x = k_0$ with increasingly negative ϵ'. It has also been observed that increasing the slab thickness from $0.4\mu m$

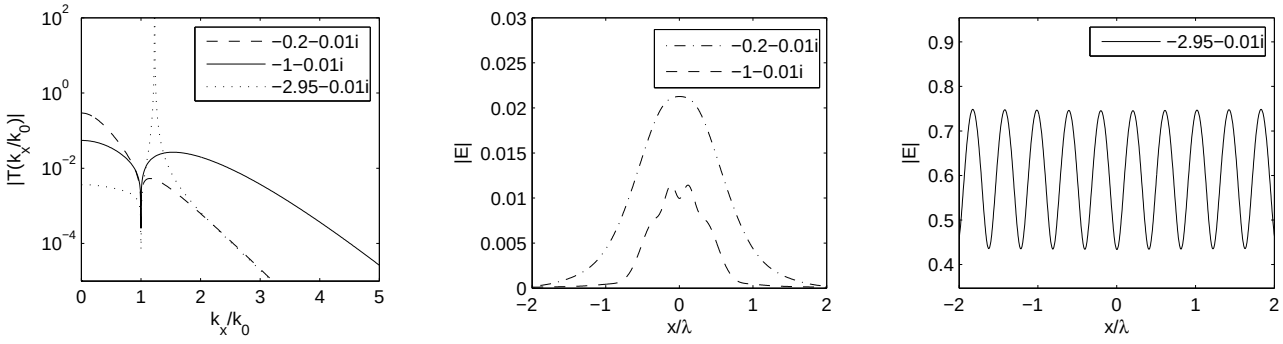

(a) (b) (c)

Figure 3: (a) The transmission spectrum ($|T|$) with varying ϵ' with $\lambda_0 = 700$ nm and for a 400 nm thick slab. The magnitude of the total electric field $|E|$ at the transmission plane for a 400 nm thick slab having permittivity for: (b)$\epsilon = -0.02 - i0.01$, $\epsilon = -1.0 - i0.01$ and (c) $\epsilon = -2.95 - i0.01$, for a single object of width $0.1\lambda_0$.

to $0.6\mu m$ greatly reduces the overall transmission ($|T|$ decreases by about a factor of about 1000). Figure 3(b) shows the magnitude of total electric field at the transmission plane for a 400 nm thick slab having $\epsilon = -0.02 - i0.01$ and $\epsilon = -1.0 - i0.01$. Figure 3(c) shows the case for $\epsilon = -2.95 - i0.01$. The image FWHM for the free space propagation case over 400 nm is 1.4 λ_0 and with only the propagating spectrum is 0.9 λ_0. The image for $\epsilon = -1.0 - i0.01$ has a FWHM of 0.9 λ_0, which is slightly better than the free space case. While the image resolution we have achieved thus far is not particularly encouraging, the spatial ripple in Figure 3(c), due to the resonant spike in Figure 3(a), is interesting.

3 References

1. V. G. Veselago, "The electrodynamics of substances with simultaneously negative values of ϵ and μ," Sov. Phys. Uspekhi **10,** 509–514 (1968).
2. J. B. Pendry, "Negative refractive index makes a perfect lens," Phys. Rev. Lett. **85,** 39663969 (2000).
3. K. J. Webb, M. Yang, D. W. Ward, and K. A. Nelson, "Metrics for negative-refractive-index materials," Phys. Rev. E **70,** 035602 (2004).
4. M. Yang and K. J. Webb, "Poynting vector analysis of a superlens," Opt. Lett. **30,** 2382–2384 (2005).
5. K. J. Webb and M. Yang, "Subwavelength imaging with a multilayer silver film structure," Opt. Lett. **31,** 2130–2132 (2006).
6. C. Luo, S. G. Johnson, J. D. Joannopoulos, and J. B. Pendry, "All-angle negative refraction without negative effective index," Phys. Rev. B **65,** 201104 (2002).
7. A. Berrier, M. Mulot, M. Swillo, M. Qiu, L. Thylén, A. Talneau, and S. Anand, "Negative refraction at infrared wavelengths in a two-dimensional photonic crystal," Phys. Rev. Lett. **93,** 073902 (2004).
8. M. Yang, J. Li, and K. J. Webb, "Functional field transformation with irregular waveguide structures," Applied Physics Lett. **14,** 2736 (2003).
9. M. Yang, H. Chen, K. J. Webb, S. Minin, S. L. Chuang, and G. R. Cueva, "Demonstration of Mode Conversion in an Irregular Waveguide," Opt. Lett. **31,** 383–385 (2006).
10. J. Li, G. J. Burke, D. A. White, C. A. Thompson, and K. J. Webb, "Design of near-field irregular diffractive optical elements using a multiresolution direct binary search method," Opt. Lett. **31,** 1181–1183 (2006).